Visible Light Induced Electron Transfer and Long-Lived Charge Separated State in Cyanine Dye/Layered Titanate Intercalation Compounds

Nobuyoshi Miyamoto[†] and Kazuyuki Kuroda[†,‡]

Department of Applied Chemistry, Waseda University, Ohkubo 3-4-1, Shinjuku-ku, Tokyo 169-8555, Japan, and Kagami Memorial Laboratory for Materials Science and Technology, Waseda University, Nishiwaseda 2-8-26, Shinjuku-ku, Tokyo 169-0051, Japan

Makoto Ogawa*

PRESTO, Japan Science and Technology Corporation, and Department of Earth Sciences, Waseda University, Nishiwaseda 1-6-1, Shinjuku-ku, Tokyo 169-8050, Japan

Received: June 8, 2003; In Final Form: September 3, 2003

Visible light induced guest-to-host electron transfer and formation of long-lived charge separated state were demonstrated in cyanine dye/layered titanate intercalation compounds. 1,1′-Diethyl-2,2′-cyanine (**dye-1**) and 5,5′-dichloro-3,3′,9-triethyl-thiacarbocyanine (**dye-2**) were intercalated into layered titanates, $Cs_xTi_{2-x/4}\square_{x/4}O_4$ ($\square$ = vacancy, $x = 0.7$) and $Na_2Ti_3O_7$, by cation exchange reactions with alkylammonium-exchanged forms as the intermediates. The formation of the intercalation compounds was confirmed by XRD, elemental analysis, and visible absorption and fluorescence spectroscopies. The intercalated dyes formed J-aggregates in the interlayer spaces for all the dye/titanate systems. The visible light induced electron transfer was shown by the appearance of ESR signal, which was ascribed to the radical dications of the dyes, and by the quenching of the fluorescence of the dye aggregates. Apparent lifetimes of the charge separated states were estimated from the decay curve of the ESR signal. The charge separated state was most stable in the **dye-2**/$Cs_xTi_{2-x/4}\square_{x/4}O_4$ system with the lifetime of 246 min among four tested compounds.

Introduction

Hybridization of wide bandgap semiconductors with sensitizing dyes is a promising way to modify the materials to be responsive to visible lights. Dye-sensitized solar cells and photocatalysts have been investigated aiming at utilizing the whole spectral range of solar light in the energy conversion systems. There have been so many publications on exploring new sensitizing dyes and complexations to construct hybrid materials. Microcrystalline semiconductor solar cells with Ru−polypyridine complexes as senstizers are known examples.[1] Materials with controlled and defined nanostructures are valuable for fundamental studies of the photoprocesses in dye-sensitized semiconductor systems to optimize the materials performance.

Because several inorganic layered solids are usable to fabricate defined and organized multilayered structures with guest species in a nanometer scale by intercalation,[2−4] the combination of sensitizing dyes with inorganic layered semiconducting solids seems to be promising for fabricating desired electron-transfer systems. Layered titanates are suitable for such purposes because of their ion-exchange capability[5,6] and semiconductivity.[7,8] A series of layered titanates with variable chemical compositions and structures are available, so that systematic studies on the physicochemical properties have been possible.[8−24]

UV light induced electron transfer in the intercalation compounds of viologens with layered semiconductors (layered niobates and titanate)[9−12,16] was reported. Visible light induced guest-to-host electron transfer was also reported. Tris(2,2′-bipyridine)ruthenium(II) complex cation (abbreviated as $[Ru(bpy)_3]^{2+}$)[14,19] was intercalated in the interlayer spaces of layered titanates and niobates, and the guest-to-host electron transfer induced by visible light was demonstrated, on the basis of the fluorescence quenching. $[Ru(bpy)_3]^{2+}$ was also adsorbed on the external surfaces of layered niobates and titanates,[8,21,22] and the sensitized photocatalytic properties were investigated. Porphyrins have also been used as sensitizers.[20,23,24] However, long-lived charge separated state of intercalation compounds induced by visible light has never been achieved, whereas the formation of unusually long-lived charge separated state was reported for $K_2La_2Ti_3O_{10}$ or the titanate doped with Pr^{3+}, Tb^{3+} (∼10 min)[17] and for layered titanates and niobates intercalated with methyl viologen (>1 h).[9−12,16] $[Ru(bpy)_3]^{2+}$ and cationic porphyrins tend to aggregate when adsorbed to layered solids,[3] and the excited state of the dyes change upon aggregation. Therefore, the sensitizers were incorporated as monomers in the reported systems. However, certain kinds of dyes such as covalently linked polynuclear complexes[25,26] and self-assembled dye aggregates[27,28] are known to show excellent sensitizing properties. The use of these dye aggregates as sensitizers in intercalation compounds would open up further variation and better properties.

In this study, we prepared cyanine dye/layered titanate intercalation compounds, where the dye formed so-called J-aggregates in the interlayer space and acted as sensitizers. The guest-to-host electron transfer was induced by visible light and unusually a long-lived charge separated state was achieved in these compounds. The layered titanates, $Na_2Ti_3O_7$ and $Cs_xTi_{2-x/4}\square_{x/4}O_4$ (Chart 1) were used as the host materials. Two

[†] Department of Applied Chemistry.
[‡] Kagami Memorial Laboratory for Materials Science and Technology.
* To whom correspondence should be addressed. Fax: 81-3-3207-4950. E-mail: makoto@waseda.jp.

10.1021/jp035617s CCC: $27.50
Published on Web 03/13/2004

CHART 1: Layered Titanates Used in This Study: (a) $Cs_xTi_{2-x/4}\square_{x/4}O_4$, and (b) $Na_2Ti_3O_7$

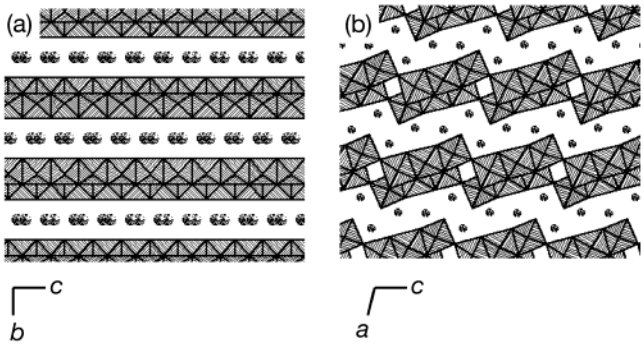

CHART 2: Dyes Used in This Study

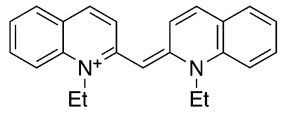

1,1'-diethyl-2,2'-cyanine bromide (**dye-1**)

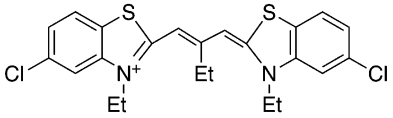

5,5'-dichloro-3,3',9-triethyl-thiacarbo cyanine bromide (**dye-2**)

cyanine dyes (Chart 2), 1,1′-diethyl-2,2′-cyanine (**dye-1**) and 5,5′-dichloro-3,3′,9-triethyl-thiacarbocyanine (**dye-2**), were employed as the guest species because they form J-aggregates and are widely used as excellent sensitizers in silver bromide based photographic systems.[27,28]

Experimental Section

Materials. 1,1′-Diethyl-2,2′-cyanine bromide (**dye-1**, purity 99.9%) and 5,5′-dichloro-3,3′,9-triethylthiacarbocyanine iodide (**dye-2**, purity 97.8%) were purchased from Hayashibara Biochemical Laboratories, Inc. and were used without further purification. The layered titanates were synthesized according to the reported solid-state reactions.[6,29,30] $Na_2Ti_3O_7$[6,29] was synthesized by heating a mixture of Na_2CO_3 and TiO_2 (anatase) in the molar ratio of 1.1:3 at 900 °C for 24 h, and then for another 24 h after grinding. $Cs_xTi_{2-x/4}\square_{x/4}O_4$[30,31] was synthesized by heating a mixture of Cs_2CO_3 and TiO_2 in the molar ratio of 1:5.2 at 800 °C for 20 h. The formation of the layered titanates was confirmed by XRD because most of the peaks coincided with those in the literatures.[6,31] Natural Na−montmorillonite (product of Tsukinuno mine, Japan; JCSS-3101, reference clay sample supplied from The Clay Science Society of Japan; its cation exchange capacity is 119 mequiv/100 g of clay) was used as received.

Intercalation of Alkylammonium Ions. Proton-exchanged layered titanates (H/Ti_3O_7 and $H/Ti_{2-x/4}\square_{x/4}O_4$) were obtained by the procedures similar to those reported previously.[6,31] The host materials were dispersed in 1 M HCl in the ratios of 10 g of host/L for $Na_2Ti_3O_7$ and 50 g of host/L for $Cs_xTi_{2-x/4}\square_{x/4}O_4$, and the mixtures were magnetically stirred for 3 days at room temperature. Hydrochloric acid was replaced every day. The powder XRD patterns of the proton-exchanged forms were similar to those reported previously, showing the successful proton exchange.[6,31]

Intercalation of propylammonium and hexylammonium ions into H/Ti_3O_7 was conducted by a two-step reaction because preintercalation of methylammonium was effective to completely remove unreacted H/Ti_3O_7 in the products.[32] H/Ti_3O_7 was sealed in a glass ampule with an aqueous solution of methylamine (40 vol %) and was allowed to react at 60 °C for 6 days to obtain a methylammonium/Ti_3O_7 intercalation compound. The methylammonium/Ti_3O_7 was allowed to react with an aqueous solution of propylamine (50 vol %) or hexylamine (50 vol %) at 60 °C for 6 days to yield propylammonium/Ti_3O_7 and hexylammonium/Ti_3O_7 intercalation compounds. Propylammonium/$Ti_{2-x/4}\square_{x/4}O_4$ was synthesized by the reaction of an aqueous solution of propylamine (50 vol %) with $H/Ti_{2-x/4}\square_{x/4}O_4$ at 60 °C for 6 days. For all the reactions, excess amounts of the alkylammonium ions (the molar ratio of alkylammonium/H in titanates = 20) were used, and the products were washed repeatedly with acetone to remove residual alkylamines.

Intercalation of the Dyes. A **dye-1**/Ti_3O_7 intercalation compound was synthesized by the reaction of the propylammonium/Ti_3O_7 intercalation compound with an aqueous solution of **dye-1** (5×10^{-5} M) at 60 °C for 6 days in a glass ampule. **Dye-2**/Ti_3O_7 was obtained by the reaction of hexylammonium/Ti_3O_7 with a **dye-2** solution (5×10^{-5} M) in the mixture of methanol and water (1 + 1 in volume). **Dye-1**/$Ti_{2-x/4}\square_{x/4}O_4$ and **dye-2**/$Ti_{2-x/4}\square_{x/4}O_4$ were synthesized by the reactions of the dye solutions with propylammonium/$Ti_{2-x/4}\square_{x/4}O_4$ under the same condition. The molar ratios of dye/[Ti_3O_7] and dye/[$Ti_{2-x/4}\square_{x/4}O_4$] in the mixtures were set to 0.3−0.45. The reaction with larger amounts of the dyes did not lead to a further increase in the adsorbed amounts of the dyes, indicating that the intercalation reaction proceeded to the point where the available interlayer space is fully occupied by the dye rather than quantitatively. Intercalation of **dye-1** and **dye-2** into Na−montmorillonite was conducted by dispersing the host in the dye solutions and stirring the mixture at room temperature for 1 day. All the samples were washed with acetone to remove residual dyes until the supernatant after centrifugation became colorless.

Characterizations. XRD patterns of the powder samples were measured on a Mac Science MXP^3 diffractometer with monochromated Cu Kα radiation. CHN analysis was performed to determine the adsorbed amounts of the alkylammonium ions and the dyes in the products with a Perkin-Elmer PE−2400II instrument. The UV−vis spectra were measured with a Shimadzu UV-2500PC spectrophotometer for aqueous suspensions containing 0.2 g/L of the powder samples. Fluorescence spectra of the suspensions were measured on a Hitachi FS-4500 fluorophotometer. The excitation wavelengths were 490 and 590 nm for the **dye-1** and **dye-2** systems, respectively. Fluorescence spectra are normally altered at higher concentrations by reabsorption of the fluorescence and scattering of excitation and fluorescence lights. To avoid such effects, the spectra were measured at the sufficiently low concentrations where such effects were negligible; the spectra of the suspensions with varied concentrations were preliminary measured to check the effects (Figure S1 of the Supporting Information). The concentrations of the dyes in the suspensions were in sufficiently narrow ranges (1.4×10^{-4} and 1.8×10^{-4} M for the **dye-1** systems and 0.8×10^{-4} and 1.2×10^{-4} M for the **dye-2** systems), allowing us to compare the fluorescence intensities. Light induced ESR spectra were taken with a JEOL JES-PX1060 electron spin resonance spectrometer under the irradiations of UV and visible lights to the powder samples. The powders were placed in the bottom of a glass tube and stored in dark before the measurements to avoid the generation of radicals by environmental illuminations. The ESR spectra were also measured under controlled temperature, using a JEOL JES-FA300

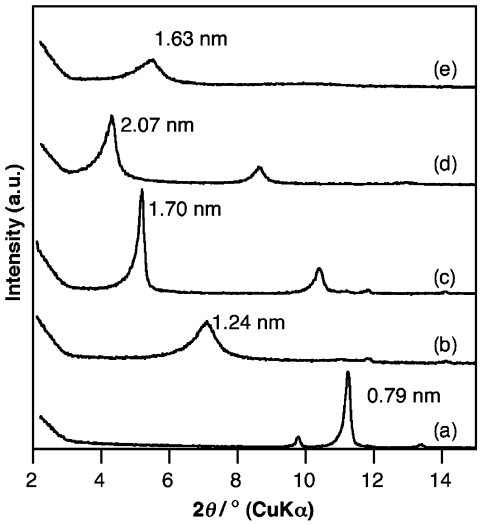

Figure 1. XRD patterns of (a) H/Ti_3O_7, (b) propylammonium/Ti_3O_7, (c) **dye-1**/Ti_3O_7, (d) hexylammonium/Ti_3O_7, and (e) **dye-2**/Ti_3O_7.

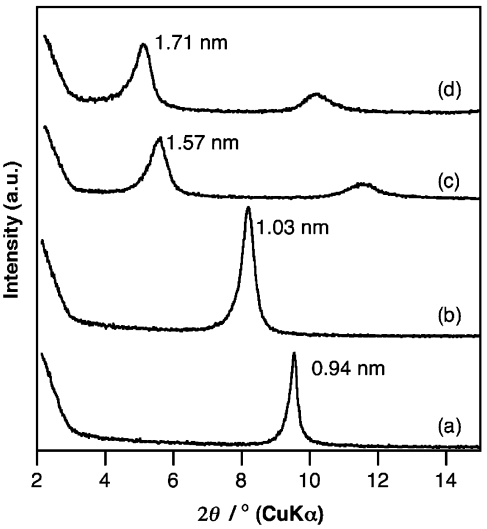

Figure 2. XRD patterns of (a) $H/Ti_{2-x/4}\square_{x/4}O_4$, (b) propylammonium/$Ti_{2-x/4}\square_{x/4}O_4$, (c) **dye-1**/$Ti_{2-x/4}\square_{x/4}O_4$, and (d) **dye-2**/$Ti_{2-x/4}\square_{x/4}O_4$.

electron spin resonance spectrometer attached with an ES-DVT4 temperature controller. The UV and visible lights were irradiated with a USHIO 100W Xe-lamp through a band-pass filter, HOYA U-340 (the transmittance centered at 350 nm), and a sharp-cut filter, HOYA L42 (cutoff wavelength is 420 nm), respectively.

Results

Syntheses of the Intercalation Compounds. The formation of the intermediates, alkylammonium-exchanged forms, was confirmed by XRD and elemental analyses. The basal spacings of propylammonium/Ti_3O_7, hexylammonium/Ti_3O_7 and propylammonium/$Ti_{2-x/4}\square_{x/4}O_4$ were 1.24 nm (Figure 1b), 2.07 nm (Figure 1d), and 1.03 nm (Figure 2b), respectively, and the values were expanded from those of the proton-exchanged forms (0.79 nm (Figure 1a) for H/Ti_3O_7 and 0.94 nm for $H/Ti_{2-x/4}\square_{x/4}O_4$ (Figure 2a)), indicating the formation of the alkylammonium-titanates intercalation compounds. The amounts of the intercalated alkylammonium ions were 0.31, 0.67, and 0.52 molecules per the formula units of the titanates for propylammonium/Ti_3O_7, hexylammonium/Ti_3O_7, and propylammonium/$Ti_{2-x/4}\square_{x/4}O_4$, respectively.

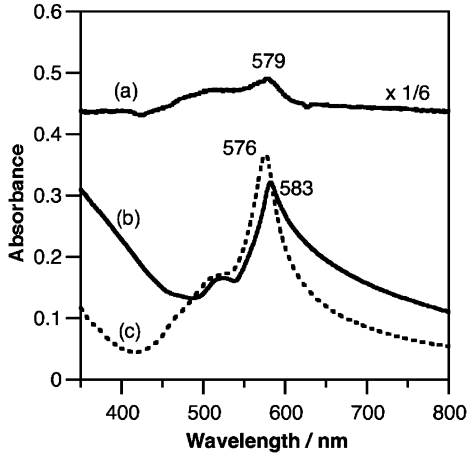

Figure 3. Visible absorption spectra of aqueous suspensions of (a) **dye-1**/Ti_3O_7, (b) **dye-1**/$Ti_{2-x/4}\square_{x/4}O_4$, and (c) **dye-1**/montmorillonite.

The XRD patterns of the dye/layered titanate intercalation compounds show that, after the reactions with the dyes, the *d* values were varied to 1.70 nm (Figure 1c), 1.63 nm (Figure 1e), 1.57 nm (Figure 2c), and 1.71 nm (Figure 2d) for **dye-1**/Ti_3O_7, **dye-2**/Ti_3O_7, **dye-1**/$Ti_{2-x/4}\square_{x/4}O_4$ and **dye-2**/$Ti_{2-x/4}\square_{x/4}O_4$, respectively, indicating the successful formation of the intercalation compounds. Supposing that all the C atoms are derived from the dyes (i.e., all the alkylammonium cations were displaced by the dyes and protons), the amounts of the adsorbed dyes were determined to be 0.20, 0.13, 0.23, and 0.14 molecules per the formula units of the hosts (or 69, 60, 89, and 45 mmol/100 g of the samples), for **dye-1**/Ti_3O_7, **dye-2**/Ti_3O_7, **dye-1**/$Ti_{2-x/4}\square_{x/4}O_4$, and **dye-2**/$Ti_{2-x/4}\square_{x/4}O_4$, respectively.

Pre-intercalation of alkylammonium ion was necessary for intercalation of the dyes in all the systems. We have already reported[32] that **dye-1** was not intercalated directly to $Na_2Ti_3O_7$ and H/Ti_3O_7 and the use of the intermediate, propylammonium/Ti_3O_7, led the successful intercalation. The use of intermediate also promoted the intercalation of the dyes into $Cs_xTi_{2-x/4}\square_{x/4}O_4$; the intercalation of **dye-1** and **dye-2** into $Cs_x/Ti_{2-x/4}\square_{x/4}O_4$ was successful when propylammonium/$Ti_{2-x/4}\square_{x/4}O_4$ was used as the host material, whereas they were not intercalated directly into $Cs_xTi_{2-x/4}\square_{x/4}O_4$ and $H/Ti_{2-x/4}\square_{x/4}O_4$. Intercalation of **dye-2** into $Na_2Ti_3O_7$ was achieved only when hexylammonium/Ti_3O_7 was used as the intermediate. The intercalation was unsuccessful when propylammonium/Ti_3O_7 was used. Higher hydrophobicity and sufficient expansion of the interlayer space are thought to be responsible for the reactivities.

The formation of the **dye-1**/montmorillonite and **dye-2**/montmorillonite intercalation compounds was shown by XRD and CHN analyses. The basal spacing increased from 1.3 nm (Na−montmorillonite) to 1.7 and 1.6 nm for the **dye-1** and **dye-2** systems, respectively; the value for **dye-1** is in accordance with the reported value, indicating the intercalation of the dye.[33] The adsorbed amounts of the dyes were determined to be 80 and 39 mmol/100 g of the **dye-1**/ and **dye-2**/montmorillonite intercalation compounds, respectively.

UV−Vis Spectra. The UV−vis absorption spectra revealed the formation of J-aggregates of the dyes in the interlayer spaces of the intercalation compounds. In the spectra of **dye-1**/Ti_3O_7 (Figure 3a), **dye-1**/$Ti_{2-x/4}\square_{x/4}O_4$ (Figure 3b), and **dye-1**/montmorillonite (Figure 3c), the sharp absorption bands were observed at around 579, 583, and 576 nm, respectively, which were remarkably red-shifted relative to the monomer band (523 nm) observed in a dilute (5×10^{-5} M) aqueous solution of

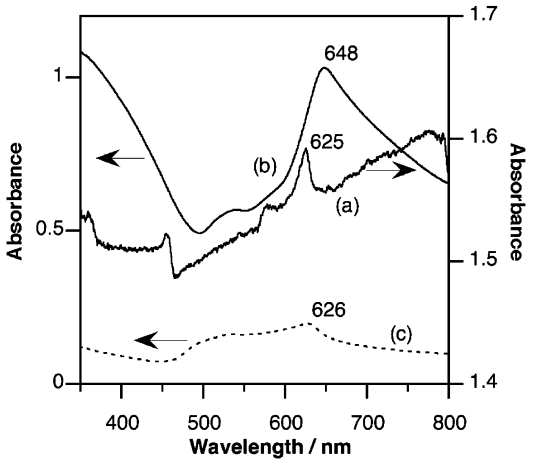

Figure 4. Visible absorption spectra of aqueous suspensions of (a) **dye-2**/Ti_3O_7, (b) **dye-2**/$Ti_{2-x/4}\square_{x/4}O_4$, and (c) **dye-2**/montmorillonite.

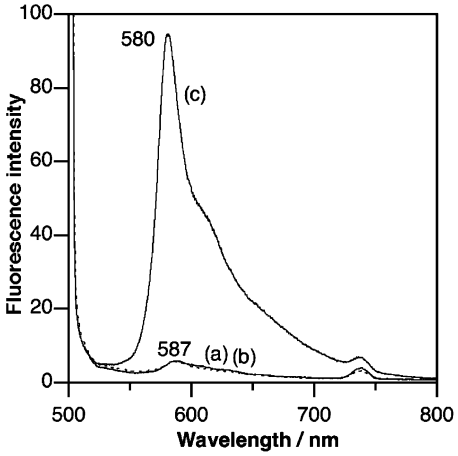

Figure 5. Fluorescence spectra of (a) **dye-1**/Ti_3O_7, (b) **dye-1**/$Ti_{2-x/4}\square_{x/4}O_4$, and (c) **dye-1**/montmorillonite.

dye-1. It is well established that J-aggregates of cyanine dyes show red-shifted absorption bands relative to the monomer bands due to exciton coupling.[27] The observed red-shifted bands (Figure 3a−c) are attributed to the J-aggregates of **dye-1**.

The formation of J-aggregates of **dye-2** in the interlayer spaces was also proved by the UV−vis spectra. Although the monomer band is observed at 553 nm in a dilute (4×10^{-6} M) methanol solution of the dye, the absorption maxima were observed at relatively longer wavelengths (648, 625, and 626 nm for **dye-2**/Ti_3O_7 (Figure 4a), **dye-2**/$Ti_{2-x/4}\square_{x/4}O_4$ (Figure 4b), and **dye-2**/montmorillonite (Figure 4c), respectively), indicating the formation of J-aggregates.

Figure 5 shows the fluorescence spectra of **dye-1**/Ti_3O_7, **dye-1**/$Ti_{2-x/4}\square_{x/4}O_4$, and **dye-1**/motmorillonite. The observed band around 587 nm (Figure 5a,b) and 580 nm (Figure 5c) are ascribed to the resonance emission from the J-aggregates. Remarkably, the fluorescence intensities were much weaker for **dye-1**/Ti_3O_7 and **dye-1**/$Ti_{2-x/4}\square_{x/4}O_4$ compared to **dye-1**/montmorillonite, indicating that the fluorescence was quenched in the titanate systems. In the **dye-2** systems, the fluorescence from the J-aggregates was observed only for **dye-2**/montmorillonite at 633 nm (Figure 6c), whereas the fluorescence was thoroughly quenched for the **dye-2**/Ti_3O_7 and **dye-2**/$Ti_{2-x/4}\square_{x/4}O_4$ systems (Figure 6a,b).

Visible Light Induced ESR Signals. The ESR spectra of **dye-1**/Ti_3O_7 and **dye-1**/$Ti_{2-x/4}\square_{x/4}O_4$ before and after the visible light irradiation are shown in Figure 7. In both the systems, the ESR signals emerged upon the irradiation of the visible light.

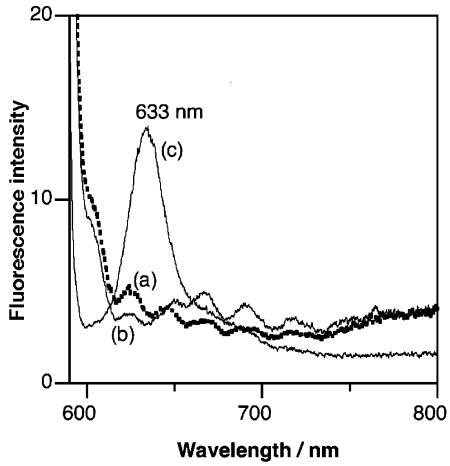

Figure 6. Fluorescence spectra of (a) **dye-2**/Ti_3O_7, (b) **dye-2**/$Ti_{2-x/4}\square_{x/4}O_4$, and (c) **dye-2**/montmorillonite.

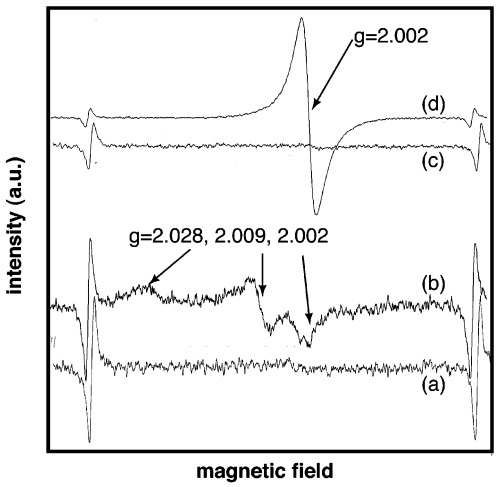

Figure 7. ESR spectra of (a), (b) **dye-1**/Ti_3O_7 and (c), (d) **dye-1**/$Ti_{2-x/4}\square_{x/4}O_4$. The spectra were measured (a), (c) before and (b), (d) after the irradiation of visible light.

The ESR signal observed for the **dye-1**/$Ti_{2-x/4}\square_{x/4}O_4$ system (Figure 7d) was isotropic with a g value of 2.002, whereas the signal was anisotropic with the peaks at $g = 2.028$, 2.009, and 2.002 for the **dye-1**/Ti_3O_7 system (Figure 7b). The g values are typical of free radicals of organic species, and light induced ESR signals[34−37] had been observed and studied in detail for various cyanine dye/AgBr systems. Therefore, the signals observed here are ascribed to dication radicals of cyanine dyes. The difference in the shapes of the spectra is thought to reflect different nanostructures of the intercalation compounds. The visible light induced ESR signals were also observed for the **dye-2** systems (Figure S2 of the Supporting Information). The spectra for the **dye-2** systems were almost isotropic with the g values of 2.002, similar to the one observed for the **dye-1**/$Ti_{2-x/4}\square_{x/4}O_4$ system.

In contrast to the above results, light induced ESR signal was not observed for the compounds without the dyes (H/Ti_3O_7, H/$Ti_{2-x/4}\square_{x/4}O_4$, propylammonium/$Ti_3O_7$ and propylammonium/$Ti_{2-x/4}\square_{x/4}O_4$) and for **dye-1**/ and **dye-2**/montmorillonite intercalation compounds. ESR signal was not observed for crystals of **dye-1** and **dye-2**. The UV light irradiation, instead of the visible light, gave only very small responses in the ESR spectra for all the dye/titanate systems.

The ESR signals began to grow just after the beginning of the irradiation and the intensity increased up to the saturation points after 15−30 min. After terminating the irradiation, the

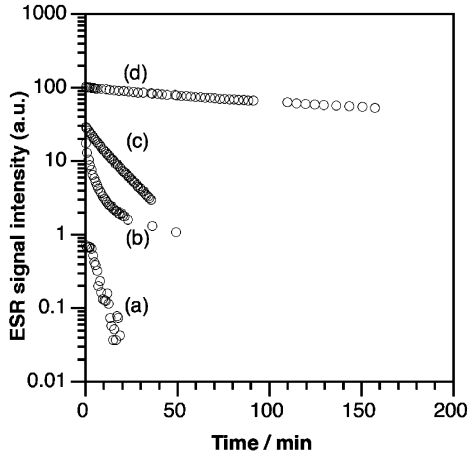

Figure 8. Decay curves of the ESR signal intensities of (a) **dye-1**/Ti_3O_7, (b) **dye-2**/Ti_3O_7, (c) **dye-1**/$Ti_{2-x/4}\square_{x/4}O_4$, and (d) **dye-2**/$Ti_{2-x/4}\square_{x/4}O_4$.

TABLE 1: Average Life Timelifetime of the Charge Separated States

sample	lifetime/min
dye-1/Ti_3O_7	6
dye-2/Ti_3O_7	22 (27%), 2 (73%)
dye-1/$Ti_{2-x/4}\square_{x/4}O_4$	17
dye-2/$Ti_{2-x/4}\square_{x/4}O_4$	246

signals immediately began to decay. The decay curves of the ESR signals in the **dye-1**/Ti_3O_7, **dye-2**/Ti_3O_7, **dye-1**/$Ti_{2-x/4}\square_{x/4}O_4$, and **dye-2**/$Ti_{2-x/4}\square_{x/4}O_4$ systems are shown in Figure 8a−d as semilog plots. By fitting the decay curves as single-exponential or double-exponential decay, we estimated the apparent lifetimes of the charge separated states, as shown in Table 1. The apparent lifetimes ranged from several minutes to hours (246 min), depending on the dye and the host: the charge separated state was more stable in the **dye-2** systems than **dye-1** systems and in the $Cs_xTi_{2-x/4}\square_{x/4}O_4$ systems than in the Ti_3O_7 systems. An N_2 purged sample was also tested for the **dye-2**/Ti_3O_7, but no remarkable difference was found in the spectrum and the decay curve is comparable to that for the sample in air.

The decay rate of the ESR signals varied depending on the temperature. Figure 9 shows the relationship (Arrhenius plot) between the temperature and the decay rate of the ESR signal intensity determined for the **dye-1**/$Ti_{2-x/4}\square_{x/4}O_4$ system. The apparent decay rate significantly dropped at lower temperature.

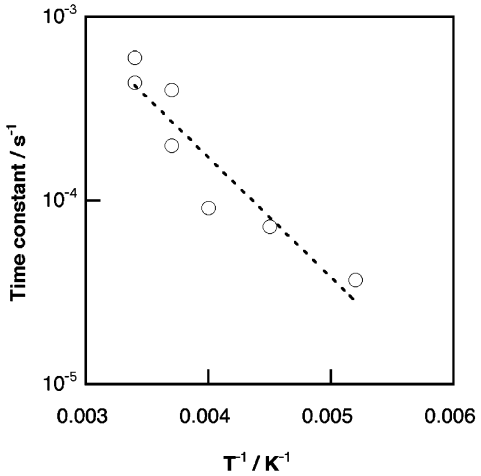

Figure 9. Relationship between reciprocal temperature and time constant of the decay of the ESR signal intensity after terminating visible light irradiation to **dye-1**/$Ti_{2-x/4}\square_{x/4}O_4$.

Discussion

Nanostructures of the Products. The nanostructures of the products are inferred from the XRD data, UV−vis spectra, and elemental analyses as well as the sizes of the dyes. The gallery height of **dye-1**/$Ti_{2-x/4}\square_{x/4}O_4$ is calculated to be 0.91 nm by subtracting the basal spacing of dehydrated H/$Ti_{2-x/4}\square_{x/4}O_4$ (0.66 nm) from the observed basal spacing (1.57 nm). Because the size of the dye is $0.4 \times 1.5 \times 0.8$ nm^3, we can derive two structural models: one is the model where the dye is present as a single molecular layer with its shorter axis of the molecular plane almost perpendicular to the titanate sheet, and the other is the model where the dye is present as a bilayer with its molecular plane parallel to the titanate sheet. Because **dye-1** is present as J-aggregate, as has been revealed by the UV−vis spectra, the single layer model is more plausible; J-aggregates of cyanine dyes are thought to possess a two-dimensional brick-stone structure where the dyes are stacked with the molecular planes flat to each other.[27] Assuming this orientation, the area occupied by the dye is estimated to be 0.24 nm^2 per the unit of $Ti_{2-x/4}\square_{x/4}O_4$. This value is comparable to the available surface area of the titanate, 0.23 nm^2 per the unit of $Ti_{2-x/4}\square_{x/4}O_4$ ($=2Zac = 2 \times 1 \times 0.383$ nm $\times$ 0.296 nm, where a and c are the lattice parameters of the titanate,[30] Z (=1) is the number of $Ti_{2-x/4}\square_{x/4}O_4$ included in a unit cell), indicating that the dyes almost fully cover the interlayer surface. We suppose that the incompatibility between the gallery height (0.91 nm) of the intercalation compound and the height of **dye-1** (0.8 nm) is due to the nanostructure of the dye aggregate; in the J-aggregate, the side chains are not on the same side, whereas the quinoline rings are overlapping,[38] resulting in the larger thickness of the aggregate layer than the height of a single dye molecule.

In the case of **dye-2**/$Ti_{2-x/4}\square_{x/4}O_4$, the intercalated amount of **dye-2** was smaller than that of **dye-1**; this is partly due to the larger size of **dye-2** ($0.3 \times 2.0 \times 0.8$ nm^3) than **dye-1**. However, the surface coverage is only 70% if we assume the orientation of the dye similar to the **dye-1** system. Judging from the fact that no larger amount of dye-2 was adsorbed by the reaction with larger amounts of the dye, the intercalation reaction should have proceeded to the point where the available interlayer space is fully covered by the dye. Supposing that the dye fully covered the layer surface, we depicted a model where the shorter molecular plane of **dye-2** is inclined by about 50° to the host layer.

Similar nanostructures are also inferred for **dye-1**/Ti_3O_7 and **dye-2**/Ti_3O_7. The gallery height is difficult to estimate for these systems because the layer is not a flat plate (Chart 1b). We roughly estimated the gallery heights as 0.91 and 0.84 nm, by subtracting the basal spacing of H/Ti_3O_7 (0.79 nm) from those of the products. Assuming that the available surface area on the titanate (0.35 nm^2 per the unit of Ti_3O_7 ($=2bc/Z = 2 \times 0.38$ nm $\times$ 0.91 nm/2, where b and c are the lattice parameters of the titanate[29] and Z (=2) is the number of Ti_3O_7 included in a unit cell)) is fully covered with the monomolecular layer of the dye, **dye-1** is packed with its shorter molecular axis almost perpendicular to the sheet, whereas **dye-2** is present with its shorter molecular axis inclined at ca. 60°, both forming J-aggregates.

We can also take into account the effect of the surface structure of the hosts on the nanostructures of the dye aggregates. We have recently showed that the surface structure of a layered niobate $K_4Nb_6O_{17}$ affects the nanostructure and the orientation of the aggregate of **dye-1**.[39] The difference in the layer structures between Ti_3O_7 and $Ti_{2-x/4}\square_{x/4}O_4$, exemplified in Chart 1, can

affect the nanostructure of the dye aggregate in the interlayers. The anisotropy of the ESR spectra observed for the **dye-1**/Ti_3O_7 system can be caused by such differences. The difference in the absorption maxima of the J-aggregates between the dye/Ti_3O_7 and dye/$Ti_{2-x/4}\square_{x/4}O_4$ systems is attributed to the difference in the size and the nanostructure (slip angle in the stacking of the dyes) of the dye according to the molecular exciton theory.[40]

Visible Light Induced Electron Transfer. The fluorescence quenching and visible light induced ESR signal strongly prove the visible light induced electron transfer from the J-aggregates of the dyes to the semiconducting host layers in all the dye/layered titanate intercalation compounds. The following photoprocesses are inferred for the present systems. The dye in the interlayer is first (1) excited by visible light and the excited dye^+* is (2) deactivated by fluorescence or (3) undergoes electron-transfer reaction to host layer to generate the conduction band electron, denoted as e^-_{CB}, followed by (4) recombination:

$$\text{Excitation of a dye:} \quad dye^+ + h\nu \rightarrow dye^+* \tag{1}$$

$$\text{Fluorescence:} \quad dye^+* \rightarrow dye^+ + \text{fluorescence} \tag{2}$$

$$\text{Electron transfer:} \quad dye^+* + \text{host} \rightarrow dye^{2+\cdot} + e^-_{CB} \tag{3}$$

$$\text{Recombination:} \quad dye^{2+\cdot} + e^-_{CB} \rightarrow dye^+ \tag{4}$$

In all the present dye/titanate systems, the ESR signals emerged with visible light irradiation, not by UV light, clearly proving the formation of $dye^{2+\cdot}$ by the processes (1) and (3), whereas the quenching of the fluorescence is interpreted as the result of the competence of fluorescence (2) with electron transfer (3). In contrast, only the processes (1) and (2) took place in the montmorillonite systems because the excited dye cannot electrically interact with the insulating aluminosilicate layers, so that neither fluorescence quenching nor ESR signals were observed. The present study thus showed a clear proof for the electron transfer from the cyanine dye J-aggregate to the semiconducting host layers. To our knowledge, this is the first case of proving light induced electron transfer between layered semiconductors and intercalated dye aggregates.

The electron transfer from the cyanine dyes to the titanate layers is energetically feasible. Although accurate potentials of the conduction band edge of the dye-intercalated titanates are unknown, it should be around the theoretically predicted values of $H_2Ti_3O_7$ (−3.54 eV vs vacuum) and $Na_2Ti_3O_7$ (−4.52 eV vs vacuum) in the literature.[22] On the other hand, the LUMO levels E_{LUMO} of **dye-1** and **dye-2** are estimated as −3.21 and −3.32 eV vs vacuum according to the electrochemically measured redox potentials E_R of the dyes[41] and the relationship[42] E_{LUMO} (eV) = $-E_R$ (V vs SCE) − 4.38.

Thus, the excited electron in the LUMO of the dyes are allowed to be transferred to the conduction band of the titanate, which is energetically lower than E_{LUMO} of the dye. Many reports on visible light induced electron transfer from cyanine dye J-aggregates to TiO_2, SnO_2, and ZnO[43] as well as to AgBr[28] also support the occurrence of the electron transfer in the present system.

Long-Lived Charge Separated States. We can discuss the kinetics of the recombination processes from the decay curves of the ESR signal intensities (Figure 8), because the ESR signal intensity is proportional to the concentration of $dye^{2+\cdot}$. Although the recombination kinetics must be rather complex than single or double exponential, the roughly estimated lifetimes shown in Table 1 indicate the high stability of the charge separated states.

Stabilization of charge separated state has been reported in some intercalation compounds containing donors or acceptors in the interlayer spaces of the semiconducting layered materials. Stabilization of methyl viologen radical dications, which were generated by photoinduced electron transfer between host and guest, were rationalized by blocking of approaching O_2, which can mediate the recombination, to the radicals.[9−12,16,44−46] However, in the present system, no remarkable difference was found in the recombination rates in N_2 and air. On the other hand, layered perovskite doped with rare earth ions exhibited luminescence even after irradiation was terminated,[17] indicating long-lived charge separated state. In that report, the slow recombination was interpreted as the slow migration of the conduction band electron due to the presence of trap sites in the host.

We suppose that the stable charge separated state observed in this study is caused by slow electron diffusion in the host layers due to the presence of trapping sites of the electron; impurities and vacant sites of the titanate should work as the trapping sites. Because the recombination rate was much slower in the $Ti_{2-x/4}\square_{x/4}O_4$ systems than in the Ti_3O_7 systems, we infer that the vacant sites in $Ti_{2-x/4}\square_{x/4}O_4$ acted as the trap sites to slow the diffusion of the conduction band electrons. Apparent activation energy of the back reaction is estimated from the slope of the Arrhenius plot (Figure 9) to be around 0.1 eV. The small activation energy can support the presence of such trap sites.[17] The nanostructure of the composites can also play an important role in the photoprocess. The higher stability of the charge separated states found for the **dye-2** systems than the **dye-1** systems would be explained by the different nanostructures of the composites as well as the difference in the energy levels of these dyes.

The J-aggregated state of the intercalated cyanine dyes should also be responsible to the long-lived charge separation. The charge left in the dye after the electron injection is regarded as a positive hole which slowly migrate in J-aggregate.[36] The migration of the positive hole would enhance spatial separation of the charges between the titanate sheet and the dye, leading to the slow back reaction. On the other hand, fast injection of the positve holes into the valence band occurs in some cyanine dye/AgBr systems when HOMO level of the dye is higher than the valence band of AgBr;[36] however, this process does not occur in the present systems, because the valence band edges of the titanates are far below the HOMO level of the dye.

Taking advantage of the further modifiable two-dimensional nanostructure of the intercalation compounds by coadsorbing other functional species in the interlayer space, the present system would be applicable as a good model system for sensitized photoenergy conversion. Further systematic study on the preparation of dye/layered titanate and niobates intercalation compounds and their optical properties are worth conducting.

Conclusions

Long-lived charge separated state induced by visible light via guest-to-host electron transfer was revealed in cyanine dye/layered titanate intercalation compounds, where the J-aggregates of the cyanine dyes effectively acted as sensitizers. The apparent lifetimes of the charge separated states ranged from several minutes to 246 min, depending on the dye and the host. The stability of the charge separated state is rationalized by slow electron diffusion in the conduction band of the hosts as well as the nanostructure of the intercalation compounds.

Acknowledgment. We thank Dr. Teruyuki Nakato (Tokyo University of Agriculture and Technology) for helpful discussion. This work was supported by a Grant-in-Aid for Scientific Research on Priority Areas (417) from the Ministry of Education, Culture, Sports, Science, and Technology (MEXT) of the Japanese Government. Waseda University also supported financially as a special research project. (2001A-537).

Supporting Information Available: The relationship between the fluorescence intensity and suspension concentration (Figure S1, PDF) and the visible light induced ESR spectra for **dye-2**/titanates (Figure S2, PDF). These materials are available free of charge via the Internet at http://pubs.acs.org.

References and Notes

(1) Hagfeldt, A.; Grätzel, M. *Acc. Chem. Res.* **2000**, *33*, 269.
(2) Ozin, G. A. *Adv. Mater.* **1992**, *4*, 612.
(3) Ogawa, M.; Kuroda, K. *Chem. Rev.* **1995**, *95*, 399.
(4) Whittingham, M. S., Jacobson, A. J., Eds.; *Intercalation Chemistry*; Academic Press: New York, 1982.
(5) Izawa, H.; Kikkawa, S.; Koizumi, M. *Polyhedron* **1983**, *2*, 741.
(6) Izawa, H.; Kikkawa, S.; Koizumi, M. *J. Phys. Chem.* **1982**, *86*, 5023.
(7) Kudo, A.; Kondo, T. *J. Mater. Chem.* **1997**, *7*, 777.
(8) Kim, Y. I.; Salim, S.; Huq, M. J.; Mallouk, T. E. *J. Am. Chem. Soc.* **1991**, *113*, 9561.
(9) Nakato, T.; Kuroda, K.; Kato, C. *J. Chem. Soc., Chem. Commun.* **1989**, 1144.
(10) Nakato, T.; Kuroda, K.; Kato, C. *Chem. Mater.* **1992**, *4*, 128.
(11) Nakato, T.; Ito, K.; Kuroda, K.; Kato, C. *Micropor. Mater.* **1993**, *1*, 283.
(12) Miyata, H.; Sugahara, Y.; Kuroda, K.; Kato, C. *J. Chem. Soc., Faraday Trans. 1* **1988**, *84*, 2677.
(13) Nakato, T.; Iwata, Y.; Kuroda, K.; Kaneko, M.; Kato, C. *J. Chem. Soc., Dalton Trans.* **1993**, 1405.
(14) Nakato, T.; Kusunoki, K.; Yoshizawa, K.; Kuroda, K.; Kaneko, M. *J. Phys. Chem.* **1995**, *99*, 17896.
(15) Nakato, T.; Kuroda, K. *Eur. J. Solid State Inorg. Chem.* **1995**, *32*, 809.
(16) Nakato, T.; Kuroda, K.; Kato, C. *Catal. Today* **1993**, *16*, 471.
(17) Kudo, A.; Sakata, T. *J. Phys. Chem.* **1995**, *99*, 15963.
(18) Kudo, A.; Kaneko, E. *Chem. Commun.* **1997**, 349.
(19) Furube, A.; Shiozawa, T.; Ishikawa, A.; Wada, A.; Domen, K.; Hirose, C. *J. Phys. Chem. B* **2002**, *106*, 3065.
(20) Kaschak, D. M.; Lean, J. T.; Waraksa, C. C.; Saupe, G. B.; Usami, H.; Mallouk, T. E. *J. Am. Chem. Soc.* **1999**, *121*, 3435.
(21) Saupe, G. B.; Mallouk, T. E.; Kim, W.; Schmehl, R. H. *J. Phys. Chem. B* **1997**, *101*, 2508.
(22) Kim, Y. I.; Atherton, S. J.; Brigham, E. S.; Mallouk, T. E. *J. Phys. Chem.* **1993**, *97*, 11802.
(23) Yamaguchi, Y.; Yui, T.; Takagi, S.; Shimada, T.; Inoue, H. *Chem. Lett.* **2001**, 644.
(24) Tong, Z.; Shichi, T.; Oshika, K.; Takagi, K. *Chem. Lett.* **2002**, *9*, 876.
(25) O'Regan, B.; Grätzel, M. *Nature* **1991**, *353*, 737.
(26) Amadelli, R.; Argazzi, R.; Bignozzi, C. A.; Scandola, F. *J. Am. Chem. Soc.* **1990**, *112*, 7099.
(27) Kobayashi, T., Ed.; *J-aggregates*; World Scientific Publishing: Singapore, 1996.
(28) Tani, T. Spectral Sensitization. In *Photographic sensitivity—Theory and mechanism*; Oxford: New York, 1995; p 111.
(29) Andersson, S.; Wadsley, A. D. *Acta Crystallogr.* **1961**, *14*, 1245.
(30) Grey, I. E.; Madsen, I. C.; Watts, J. A.; Bursil, L. A.; Kwiatkowska, J. *J. Solid State Chem.* **1985**, *58*, 350.
(31) Sasaki, T.; Watanabe, M.; Michiue, Y.; Komatsu, Y.; Izumi, F.; Takenouchi, S. *Chem. Mater.* **1995**, *7*, 1001.
(32) Miyamoto, N.; Kuroda, K.; Ogawa, M. *Mol. Cryst. Liq. Cryst.* **2000**, *341*, 259.
(33) Ogawa, M.; Kawai, R.; Kuroda, K. *J. Phys. Chem.* **1996**, *100*, 16218.
(34) Needler, W. C.; Griffith, R. L.; West, W. *Nature* **1961**, *191*, 902.
(35) Tani, T. *Photogr. Sci. Eng.* **1975**, *19*, 356.
(36) Tani, T. *J. Imaging Sci.* **1986**, *30*, 41.
(37) Tani, T. *J. Appl. Phys.* **1987**, *62*, 2456.
(38) Yoshioka, H.; Nakatsu, K. *Chem. Phys. Lett.* **1971**, *11*, 255.
(39) Miyamoto, N.; Kuroda, K.; Ogawa, M. *J. Am. Chem. Soc.* **2001**, *123*, 6949.
(40) McRae, E. D.; Kasha, M. *J. Chem. Phys.* **1958**, *28*, 721.
(41) Lenhard, J. R. *J. Imaging Sci.* **1986**, *30*, 27.
(42) Tani, T. *Photogr. Sci. Eng.* **1970**, *14*, 72.
(43) Yonezawa, Y.; Kurokawa, H.; Ito, S.; Yamamoto, M. *J. Soc. Photogr. Sci. Technol. Jpn.* **1992**, *55*, 169.
(44) Vermeulen, L. A.; Thompson, M. E. *Chem. Mater.* **1994**, *6*, 77.
(45) Vermeulen, L. A.; Thompson, M. E. *Nature* **1992**, *358*, 656.
(46) Vermeulen, L. A.; Snover, J. L.; Sapochak, L. S.; Thompson, M. E. *J. Am. Chem. Soc.* **1993**, *115*, 11767.